

Density measurements of noncrystalline materials at high pressure with diamond anvil cell

Xinguo Hong^{a)}

Consortium for Advanced Radiation Sources, University of Chicago, Chicago, Illinois 60637, USA
and MacCHESS, Cornell High Energy Synchrotron Source, Cornell University, Ithaca, New York 14853, USA

Guoyin Shen

HP-CAT, Geophysical Laboratory, Carnegie Institution of Washington, Argonne, Illinois 60439, USA

Vitali B. Prakapenka

Consortium for Advanced Radiation Sources, University of Chicago, Chicago, Illinois 60637, USA

Mark L. Rivers and Stephen R. Sutton

Consortium for Advanced Radiation Sources, University of Chicago, Chicago, Illinois 60637, USA
and Department of Geophysical Sciences, University of Chicago, Chicago, Illinois 60637, USA

(Received 5 February 2007; accepted 17 September 2007; published online 12 October 2007)

We describe an x-ray absorption method for *in situ* density measurement of non-crystalline materials in the diamond anvil cell using a monochromatic synchrotron x-ray microbeam. Sample thickness, which is indispensable in the absorption method, can be determined precisely by extrapolating the thickness profile of the gasket obtained by x-ray absorption and diffraction measurements. Diamond deformation across the sample chamber becomes noticeable at high pressures above 10 GPa, which can be monitored with a precision better than 1%, as demonstrated by measurements on crystalline Ag. We have applied the developed method to measure densities of the classic network-forming GeO₂ glass in octahedral form at pressures up to 56 GPa. The fit to the pressure-volume data with the Birch-Murnaghan equation from 13 to 56 GPa gives parameters of $V_0=23.2\pm 0.4$ cm³/mol and $K=35.8\pm 3.0$ GPa, assuming that $K'=4$. This method could be applicable for *in situ* determination of the density of liquids and other noncrystalline materials using a diamond anvil cell up to ultrahigh pressures. © 2007 American Institute of Physics. [DOI: 10.1063/1.2795662]

INTRODUCTION

Densities of noncrystalline materials, such as liquids and amorphous solids, under high pressure and temperature are of general importance in physics, materials science, and earth sciences. Density-driven or entropy-driven polyamorphism in amorphous materials has recently attracted attention.^{1–4} In the earth sciences, densities of silicate melts at high pressure are essential for understanding magma migration in planetary interiors, while densities of iron and iron-alloy liquids are required for modeling core composition and dynamics.

With the advent of brilliant synchrotron monochromatic microbeams, x-ray diffraction provides a direct and highly accurate way to measure lattice volumes or densities of crystalline phases with sample sizes down to a few microns as a function of pressure and temperature to ultrahigh pressures. In contrast, density measurement of noncrystalline materials poses special challenges because of the limited methods currently available under the spatial confinement of pressurized environments. Density determination of noncrystalline materials has been limited to a few systems at relatively low pressures. Extending the accessible pressure range with the

use of the diamond anvil cell (DAC) becomes desirable for studying the compression behavior of noncrystalline materials.

The frequently used methods using the large volume press (LVP) are based on the density dependence of x-ray absorption in a regular shaped material in pressure ranges of 0–5 GPa and temperatures of 300–900 K.^{5,6} For example, a ruby cylinder was used as a sample container so as to overcome effects of deformation of the sample shape under pressure.⁵ The density was determined from the intensity profile of transmitted x rays by means of x-ray absorption. Using a Paris-Edinburgh press, the density of FeS in the pressure and temperature ranges of 1.5–6.2 GPa and 1500–1780 K was measured.⁷ Recently a new technique of high-pressure tomography using modified Drickamer anvil apparatus was introduced for inclusion studies under pressure and temperature, and the compression behavior of vitreous Mg₂SiO₄ sphere in FeS matrix was reported up to 5 GPa.⁸ Among other methods employing the LVP is the falling sphere method,^{9,10} with probing spheres of known density placed in the sample, from which sample density is bracketed.¹⁰ However, this method is time consuming and has limited precision.

Recently, efforts have been made with the DAC. Density determination of water and argon was evaluated up to 1.1 GPa using structural data.¹¹ Densities of molten indium

^{a)} Author to whom correspondence should be address. FAX: (607)255-9001.
Electronic mail: xh48@cornell.edu

up to 8.5 GPa were measured by the x-ray absorption method with a dual hole configuration.¹² It has been pointed out¹³ that large uncertainties are inevitably involved in determining density from structural data. The x-ray absorption method is promising, but with a dual hole configuration, it requires large diamond culet size and assumes negligible thickness difference between the dual holes, thus limiting the application only at low pressures (<10 GPa). It is the goal of this paper to extend the x-ray absorption method and to introduce a procedure suitable for *in situ* density measurement at pressures much greater than 10 GPa.

With the new method, we have measured the densities of GeO₂ glass at high pressures up to 56 GPa. The results on compression of six-coordinated GeO₂ glass is reported, which can be only obtained with *in situ* measurements. Although the present example is focused on amorphous solids, the method should be applicable to structural studies of liquids as well.

EXPERIMENT AND METHOD

According to the absorption law, the x-ray transmission intensity can be written as

$$I_S = I_0 \exp(-\mu_S \rho_S d_S - \mu_D \rho_D d_D), \quad (1)$$

where I_0 is the normalized incident intensity, μ is the linear absorption coefficient, ρ is the density, d is the thickness, and subscripts S and D represent the sample and diamond anvils, respectively. If the monochromatic x-ray energy is >1 keV from any absorption edges, the thickness of gasket d_g can then be expressed by

$$d_g = [\ln(I_0/I_g) + \mu_D \rho_D d_D] / \mu_g \rho_g, \quad (2)$$

where subscript g represents the DAC gasket. The quantities on the right side of Eq. (2) are either known values (μ) or measurable (d_D , ρ , and I). The incident and transmitted x-ray intensities can be directly measured; the mass absorption coefficients (μ) are obtained from the tabulations of Elam *et al.*;¹⁴ the thickness of diamond anvils (d_D) can be directly measured; and the density of the crystalline Mo or Re gasket was calculated from x-ray diffraction measurements using the Rietveld refinement software package GSAS.¹⁵

At pressures over 10 GPa, diamond deformation occurs in the culet area,¹⁶ resulting in an uneven thickness across the sample area. To overcome the effect of bevelled and curving anvils on the density determination at high pressure, we have determined the thickness profile in the gasket region according to Eq. (2), and interpolated the profile to the sample center for sample thickness. Crystalline Ag was used as a standard for measuring the deformation of diamond anvils under high pressures and for cross-checking the accuracy of thickness determination from the interpolation. It was found that diamond deformation across the sample chamber at high pressure becomes significant above 10 GPa. The thickness profiles of the sample and the gasket at the sample center in the DAC was measured with relative errors of less than 1%. According to Eq. (1), we can determine sample density (ρ_s) using the calculated sample thickness (d_s) and known mass absorption coefficients.

Three sets of x-ray experiments have been performed on density measurements using the DAC at the GSECARS 13ID-D, 13BM-D, and HPCAT 16ID-B beamlines, Advanced Photon Source, Argonne National Laboratory. The first set of experiments had two configurations: one with a Re gasket and Ag as the sample (Re–Ag) and the other with a Mo gasket and Ag as the sample (Mo–Ag). These experiments were designed to monitor deformation of the diamond anvils under high pressure. The second set of experiments, with a Mo gasket, a Ag insert ring, and an amorphous GeO₂ sample (Mo–Ag–GeO₂) (Fig. 1), was designed to develop an optimal configuration with which the thickness profile determined from gasket can be cross-checked using the Ag ring and the sample thickness at the central position can be determined with confidence. The soft Ag ring (bulk modulus: 100 GPa) also helps to reduce the pressure gradient across the sample chamber. The third set of experiments was designed to apply the developed technique for measuring the equations of state (EOS) of GeO₂ glass in octahedral form with several DACs with different culet sizes at pressures up to 56 GPa.

In the first set experiments at the 13ID-D, diamond anvils of 300 μm culet size were used. Intense monochromatic x-radiation with fixed energy at 37.077 keV was used for x-ray absorption and diffraction measurements. The x-ray beam was focused down to a beam size of 3(vertical) \times 4(horizontal) μm at the full width at half maximum (FWHM) using Kirkpatrick-Baez (KB) mirrors.¹⁷ The x-ray intensities before and after the DAC were monitored by an Ar-filled ion chamber and a photodiode, respectively. The photodiode reading reflects the x-ray absorption of the sample and the DAC, while the reading from the ion chamber is used for normalization. The angle-dispersive x-ray diffraction measurements were performed by scanning the sample and gasket in steps of 5 μm and collecting the diffraction patterns with a high-resolution MAR CCD-165 x-ray area detector. Densities of the crystalline Ag, Re, or Mo were obtained from the lattice parameters determined by fitting the observed diffraction peaks. Pressures were determined using the pressure-dependent fluorescence of small ruby balls (<5 μm) positioned at the corner of the sample chamber.

In the second set of the Mo–Ag–GeO₂ experiments, large culet sizes of 800 μm were used to reduce pressure gradients and diamond deformation at the sample positions. Slotted WC seats were employed at both sides of the DAC, ensuring access to large angles (25°) for the incident and diffracted x-ray beams. Silver was placed in the 200 μm diameter hole of a preindented Mo gasket of 38 μm in thickness, and indented to form a unified Mo–Ag gasket. A new hole of 80 μm diameter was then drilled at the center of Mo–Ag gasket (Fig. 1). GeO₂ glass was loaded into the sample chamber without pressure medium. The GeO₂ glass is the same as that used in Ref. 18. GeO₂ glass was prepared by placing the Pt capsule containing GeO₂ powder \sim 99.999%, Alfa Aesar, inside an oven at 1390 °C, i.e., above the melting point (1086 °C), for 12 h, followed by air quenching to room temperature. The amorphous structure was verified by x-ray diffraction and Raman scattering.

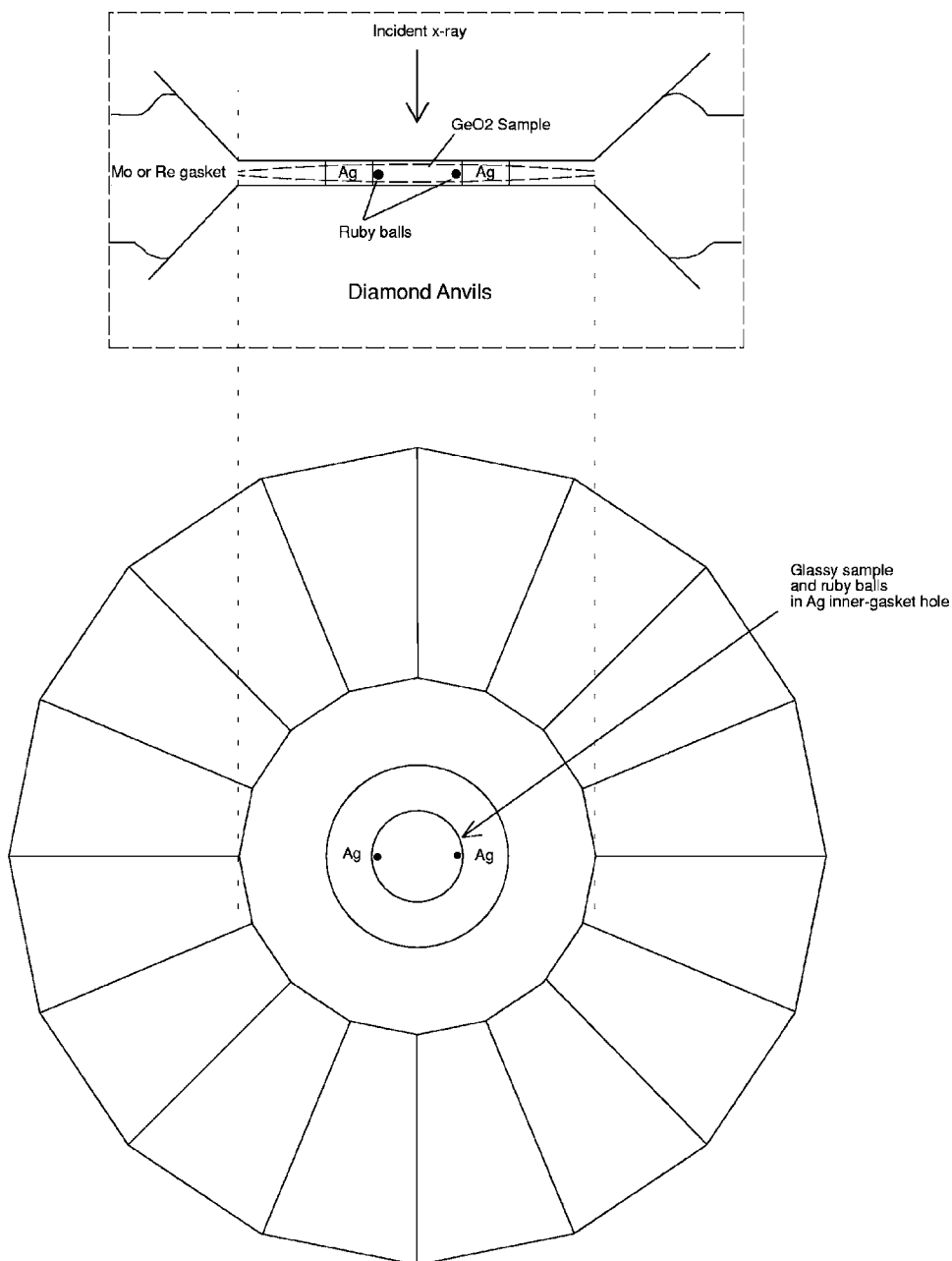


FIG. 1. Side and top views of the one-hole configuration for density measurement in the Mo–Ag–GeO₂ experiment. For the Re–Ag and Mo–Ag experiments, Ag sample fills the entire hole of the Re or Mo gasket. Dashed lines in the side view illustrate the diamond deformation at high pressure.

In the last set of experiments, different DACs with anvils of 300, 500, and 800 μm culet sizes were employed in measurements of the EOS of the octahedral form of GeO₂ glass at high pressures. Amorphous GeO₂ powder was loaded into the sample chamber of a Re or Mo gasket approximately 80 μm in diameter and 35–40 μm in thickness. To cross-check the density data of the GeO₂ glass, additional x-ray absorption and diffraction measurements were performed with 18.000 and 30.000 keV incident x rays at GSECARS 13BM-D, and 29.210 keV at HPCAT 16ID-B. The diffraction patterns of the samples and gaskets were recorded with a high-resolution MAR-345 imaging plate (IP) area detector. Simultaneous x-ray diffraction measurements were also used to document structural transitions. X-ray absorption was measured at different angles of 0° and $\pm 20^\circ$, to monitor and eliminate the influence of diamond diffraction.

RESULTS AND DISCUSSION

Figure 2(a) shows an x-ray transmission profile from the Re–Ag experiment (Fig. 1) at 20 GPa across the diamond culet using a step of 5 μm . The absorption profile of the Re gasket shows a remarkable concave shape arising from gasket densification and diamond deformation under high pressure. The transmission anomalies located at the two edges of sample hole are due to the absorption of the ruby chips. The corresponding density distribution obtained from the diffraction data of Re and Ag is shown in Fig. 2(b). Data at the edge regions were omitted due to the mixed contribution of Re, Ag, and ruby, as judged by diffraction patterns and the anomalies in absorption profiles. At 20 GPa, the density of the Re gasket shows a progressive 2.5% increase from the edge to the sample hole, while the relative variation of the Ag density in the sample hole is less than 0.3%.

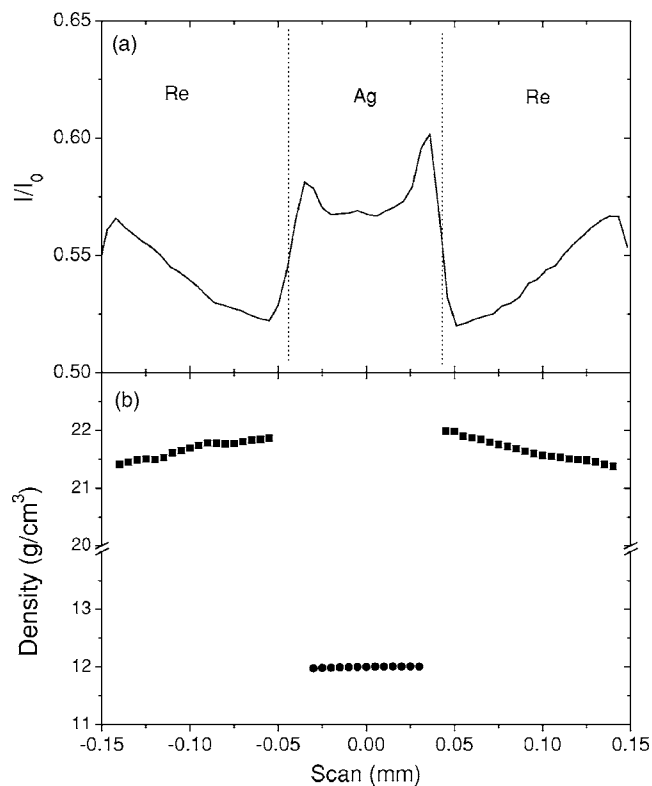


FIG. 2. (a) X-ray transmission profile in the Re–Ag experiment at 20 GPa across the diamond culet ($300\ \mu\text{m}$), measured by a photodiode and an ion chamber with a monochromatic x-ray beam at 37.077 keV. The profile was obtained by scanning the sample position with a step of $5\ \mu\text{m}$ with an x-ray beam size of $3 \times 4\ \mu\text{m}^2$ at the FWHM. Pressure was determined by ruby chips at the corner of sample hole, which is noticeable in the transmission profile at the hole edges. (b) Density distributions of Re and Ag across the DAC culet obtained from the x-ray diffraction data and GSAS fitting (Ref. 15).

It has been reported that, in the pressure range below 10 GPa, the anvil deformation was found to be negligible. At multimegabar pressures, large elastic strain at the diamond tip has been observed.¹⁶ With the small synchrotron probe, it is now possible to measure the diamond deformation under loading in detail. Such information is essential for extending the density measurements using the DAC to extremely high pressures. With the density and x-ray absorption data, the one-dimensional thickness profile between the two diamond anvils can be determined by applying Eq. (2). The profile of thickness reflects the anvil deformation under high pressure. Figure 3 shows the obtained two thickness profiles at the gasket and the sample (Ag) areas across the diamond culet at 20 and 40 GPa, respectively. With increasing pressure, diamond deformation increases. Larger deformation of the diamond anvils is observed at 40 GPa with a difference of $5.8\ \mu\text{m}$ between the central area and the culet edge, compared to $2.9\ \mu\text{m}$ at 20 GPa. This deformation represents 33% and 13% difference in thickness at 40 and 20 GPa, respectively. It is clearly shown that diamond deformation must be calibrated for a precise density measurement. Fortunately, because of the radially symmetric configuration of the conventional axial geometry in a DAC experiment, the obtained thickness across the DAC culet exhibits a simple symmetrical curve along the loading axis, making it possible to inter-

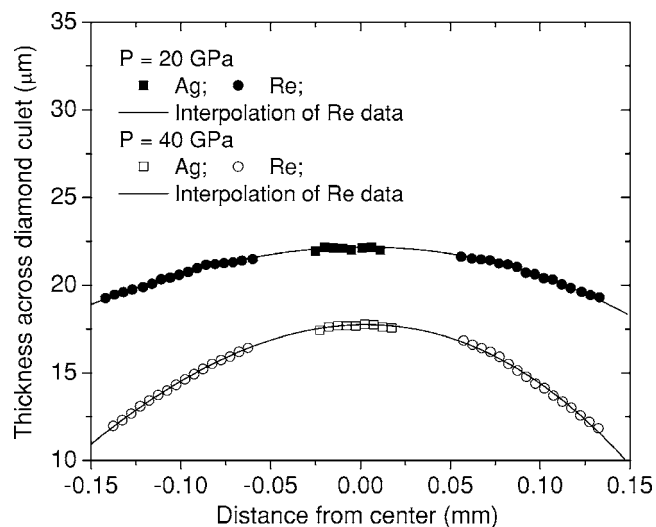


FIG. 3. Thickness of the Re gasket and Ag sample across the diamond culet. Thickness was determined using Eq. (2). The solid line is the cubic fitted curve to gasket thickness (solid or open circles). The thickness values obtained from Ag (solid or open squares) agree well with the interpolated lines, with a relative error of less than 0.5%.

polate the central sample thickness from the thickness profile of the gasket. The solid lines in Fig. 3 are the cubic polynomial fitted curves to the gasket thickness only, showing excellent consistency with those determined independently by crystalline Ag at the sample positions, at both 20 and 40 GPa. The difference between the fitted curve and the measured data for the Ag sample at the center is less than 0.5%, verifying the validity and accuracy of the sample thickness determination by interpolating the gasket thickness data. Precise sample thickness is crucial for the density measurement of noncrystalline materials using a combination of x-ray absorption and diffraction techniques.

In the interpolating method, there is an assumption that the deformation of the diamond surface under high pressure is continuous. To satisfy this assumption, it is required to carefully select diamond anvils with flat surfaces and without any visible defects. For the present study, a continuous pressure-induced diamond deformation was found (Figs. 3 and 4). Under ultrahigh pressure where the brilliant-cut DAC might be employed, reversal of curvature across the entire diamond culet may occur.¹⁶ Using a submicron x-ray beam, it would be feasible to obtain precise simple thickness measurements if only the inner culet is used in the interpolating process.

It should be noted that the accuracy of the thickness measurement is tied to the accuracy of absorption coefficients used in this study.¹⁴ In addition, the effect of deviatoric stress on the accuracy of the density measurements of the silver and rhenium gasket was not taken into account. The real gasket density may be slightly greater than the measured density, but the effect was found to be small as illustrated by the results of the Re–Ag and Mo–Ag experiments. The method introduced here could be applicable to other DAC experiments where the thickness of the sample is an important experimental parameter, e.g., ultrasonic interferometry,¹⁹ refractive index,²⁰ and conduction measurements.

To establish the relationship between culet size and the

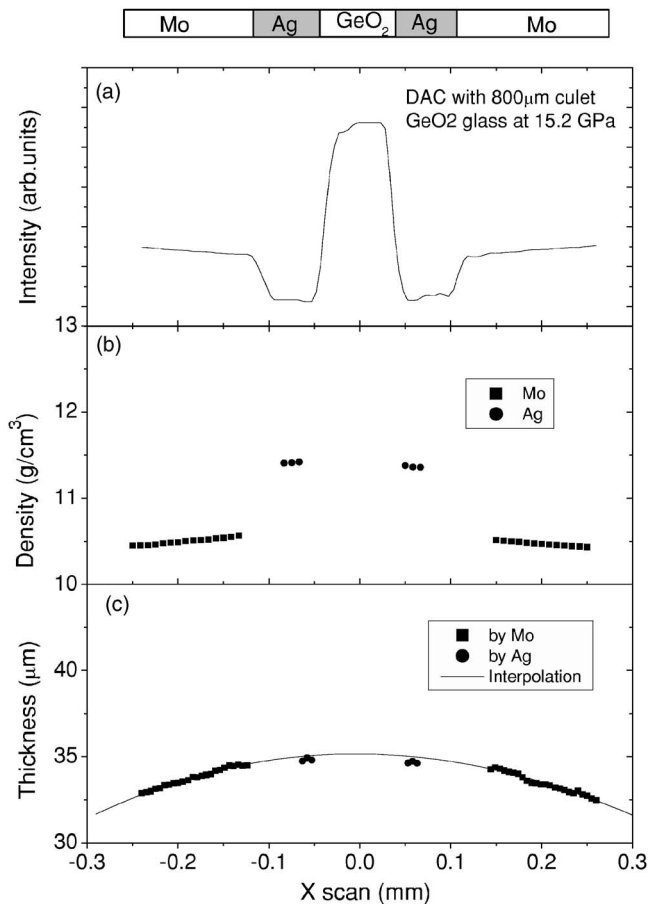


FIG. 4. (a) X-ray transmission profiles across the diamond culet in the Mo–Ag–GeO₂ experiment at 15.2 GPa. (b) The density distribution of Mo and Ag are shown as a function of radial distance across the culet [Fig. 4(b)]. The obtained thickness of the Mo gaskets [Fig. 4(c)] was fitted by the cubic polynomial curve, which is employed to interpolate the central sample thickness at the GeO₂ glass sample, being in good agreement with that of Ag calibrator. Much smaller deformation at the same distance from the DAC center was found for the diamond anvils with 800 μm culet size than that of the DAC with 300 μm culet size (Fig. 3). Unfortunately, in the experiments with 800 μm culet size, we found tiny samples retained at the Ag ring region, indicated by bumps in the transmission measurements. Such points were removed based on clear ripples in the absorption profiles in the Ag ring region [Fig. 4(a)]. Nevertheless, the remaining points show a relative deviation of less than 1% from the cubic polynomial fitting curve of the Mo gasket data.

extent of diamond anvil deformation, we used a DAC of 800 μm culet size (Fig. 1). In this Mo–Ag–GeO₂ experiment, an Ag ring was introduced as a calibrator for both the density and thickness profiles. Density distributions of Mo and Ag are shown as a function of radial distance across the culet [Fig. 4(b)]. The obtained thickness of the Mo gaskets [Fig. 4(c)] was fitted by the cubic polynomial curve, which is employed to interpolate the central sample thickness at the GeO₂ glass sample, being in good agreement with that of Ag calibrator. Much smaller deformation at the same distance from the DAC center was found for the diamond anvils with 800 μm culet size than that of the DAC with 300 μm culet size (Fig. 3). Unfortunately, in the experiments with 800 μm culet size, we found tiny samples retained at the Ag ring region, indicated by bumps in the transmission measurements. Such points were removed based on clear ripples in the absorption profiles in the Ag ring region [Fig. 4(a)]. Nevertheless, the remaining points show a relative deviation of less than 1% from the cubic polynomial fitting curve of the Mo gasket data.

Although the sample thickness can be precisely determined by the process described above, we found that strong diffraction from the single crystal diamond anvils may contribute considerable uncertainties in the absorption measurements if the Bragg condition is inadvertently satisfied. To

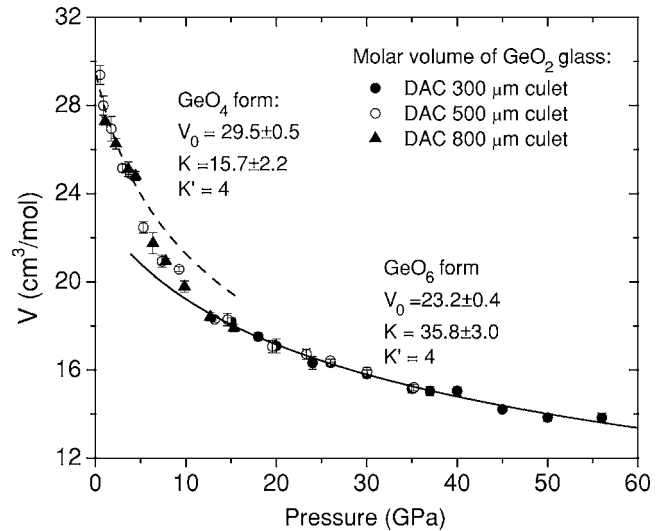


FIG. 5. Molar volumes of GeO₂ glass as a function of pressure. Different symbols indicate different experiment runs. Solid and dashed lines are the fits at the pressure range of [0.5 GPa, 4.4 GPa] and [13.2 GPa, 56 GPa] with the third-order Birch-Murnaghan equation for tetrahedral and octahedral forms, respectively.

avoid effects of diamond diffraction, the measurements of x-ray absorption and diffraction were performed at different angles of 0° and ±20°, which were selected by rotating the DAC and checking if the diffraction peaks from the diamond anvils completely disappeared from the CCD or IP image. The angle of 0° was set based on the best image measured at the initial DAC angles of 0° and ±0.5°. In some cases, slight variation in x-ray energy might be necessary to obtain a clean diffraction pattern at 0°. Once the optimum angles are determined, it is helpful to position the cleanup slits (typically 20 μm at 13-IDD and 30 μm at 13-BMD) as close to the DAC as possible so as to avoid additional scattering x-ray into the detector. Multiple measurements of x-ray absorption at different angles can effectively eliminate the influence of diamond diffraction.

Figure 5 shows the molar volumes of GeO₂ glass as a function of pressure up to 56 GPa. The molar volume data display slight scattering for several runs using different DACs (squares, circles and triangles). The variations from multiple measurements at different angles are indicated by the error bars. As shown in Fig. 5, at pressures below 4.4 GPa and above 13 GPa, GeO₂ glass exhibits elastic compression behavior, and were fitted to the Birch-Murnaghan equation of state,²¹

$$P = \frac{3}{2}K_0 \left[\left(\frac{V}{V_0} \right)^{-7/3} - \left(\frac{V}{V_0} \right)^{-5/3} \right] \times \left\{ 1 - \frac{3}{4}(4 - K') \left[\left(\frac{V}{V_0} \right)^{-2/3} - 1 \right] + \dots \right\}, \quad (3)$$

where V and V_0 are the volume at P and 1 bar, respectively, K_0 is the bulk modulus, and K' is the pressure derivative of K_0 . The solid line in Fig. 5 represents a fit for the octahedral glass with the Birch-Murnaghan equation to the pressure-volume data from 13 to 56 GPa. It gives $V_0 = 23.2 \pm 0.4$ cm³/mol and $K_0 = 35.8 \pm 3.0$ GPa, assuming that $K' = 4$. The same fitting process for the tetrahedral data

(dashed line) from 0.5 to 4.4 GPa gives $V_0=29.5\pm 0.5$ cm³/mol and $K_0=15.7\pm 2.2$ GPa, assuming that $K'=4$. The compression behavior (EOS) of GeO₂ glass has been studied by ultrasonic techniques to 6 GPa,²² optical methods to 7.1 GPa,²³ and strain-gauge techniques to 9 GPa,²⁴ covering approximately half of the coordination change region of 4–13 GPa defined by different techniques.^{23,25–27} The density of GeO₂ glass measured by optical,²³ strain-gauge,²⁴ Brillouin,²⁸ and ultrasonic techniques²² exhibits, however, considerable discrepancies between these data at pressures above 5 GPa. In Ref. 17 we have compared our low-pressure density data with the published values, being in good agreement with the tetrahedral GeO₂ glass. The bulk modulus K_0 in the Birch-Murnaghan fit for the octahedral form is more than twice that of the tetrahedral form, while V_0 decreases to about 21%.

In summary, we have introduced a method for precisely measuring sample thickness *in situ* at high pressure in the DAC, which is crucial for the density measurement of non-crystalline materials using x-ray absorption and diffraction techniques. Diamond deformation across the sample chamber at high pressure can be measured with a relative error of less than 1%. For GeO₂ glass, the density data have been obtained at pressures up to 56 GPa. Thus, the method could be used for studies of pressure-induced polyamorphism in noncrystalline materials and the equations of state of liquid iron and silicate melts at conditions relevant to the interiors of the Earth and other planets. In the future, with the reduction of x-ray beam size to the submicron range, density measurements above 1 Mbar should be feasible.

ACKNOWLEDGMENTS

The author would like to thank M. Newville for assistance in the experiment. This work was supported by NSF-EAR Grant No. 0229987. The GSECARS sector is supported by the NSF (Earth Sciences Instrumentation and Facilities Program) and DOE (Geoscience Program). Use of the HP-CAT facility is supported by DOE-BES, DOE-NNSA.

¹D. A. Young, *Phase Diagrams of the Elements* (University of California Press, Berkeley, 1991).

²C. J. Roberts, A. Z. Panagiotopoulos, and P. G. Debenedetti, *Phys. Rev. Lett.* **77**, 4386 (1996).

- ³A. C. Wright, G. Etherington, J. A. E. Desa, R. N. Sinclair, G. A. N. Connell, and J. Mikkelsen, *J. Non-Cryst. Solids* **49**, 63 (1982).
- ⁴P. F. McMillan, *High Pressure Phenomena (Fenomeni ad Alte Pressioni)* (IOS, Amsterdam, 2002).
- ⁵Y. Katayama, *High Press. Res.* **14**, 383 (1996).
- ⁶Y. Katayama, K. Tsuji, O. Shimomura, T. Kikegawa, M. Mezouar, D. Martinez-Garcia, J. M. Besson, D. Hausermann, and M. Hanfland, *J. Synchrotron Radiat.* **5**, 1023 (1998).
- ⁷C. Sanloup, F. Guyot, P. Gillet, G. Fiquet, M. Mezouar, and I. Martinez, *Geophys. Res. Lett.* **27**, 811 (2000).
- ⁸Y. Wang, T. Uchida, F. Westferro, M. L. Rivers, N. Nishiyama, J. Gebhardt, C. E. Leshner, and S. R. Sutton, *Rev. Sci. Instrum.* **76**, 073709 (2005).
- ⁹C. B. Agee and D. Walker, *J. Geophys. Res.* **93**, 3437 (1988).
- ¹⁰R. A. Secco, R. F. Tucker, S. P. Balog, and M. D. Rutter, *Rev. Sci. Instrum.* **72**, 2114 (2001).
- ¹¹J. H. Eggert, G. Weck, P. Loubeyre, and M. Mezouar, *Phys. Rev. B* **65**, 174105 (2002).
- ¹²G. Shen, N. Sata, M. Newville, M. L. Rivers, and S. R. Sutton, *Appl. Phys. Lett.* **81**, 1411 (2002).
- ¹³G. Shen, M. L. Rivers, S. R. Sutton, N. Sata, V. B. Prakapenka, J. S. Oxley, and K. S. Suslick, *Phys. Earth Planet. Inter.* **143–144**, 481 (2004).
- ¹⁴W. T. Elam, B. Ravel, and J. R. Sieber, *Radiat. Phys. Chem.* **63**, 121 (2002).
- ¹⁵A. C. Larson and R. B. Von Dreele, Los Alamos National Laboratory, Report No. LAUR 86-748, 2000, <http://www.ncnr.nist.gov/programs/crystallography/software/gsas.html>.
- ¹⁶R. J. Hemley, H.-k. Mao, G. Shen, J. Badro, P. Gillet, M. Hanfland, and D. Hausermann, *Science* **276**, 1242 (1997).
- ¹⁷G. Shen, V. B. Prakapenka, P. J. Eng, M. L. Rivers, and S. R. Sutton, *J. Synchrotron Radiat.* **12**, 642 (2005).
- ¹⁸X. Hong, G. Shen, V. B. Prakapenka, M. Newville, M. L. Rivers, and S. R. Sutton, *Phys. Rev. B* **75**, 104201 (2007).
- ¹⁹W. A. Bassett, H.-J. Reichmann, R. J. Angel, H. Spetzler, and J. R. Smyth, *Am. Mineral.* **85**, 283 (2000).
- ²⁰C.-s. Zha, R. J. Hemley, H.-k. Mao, T. S. Duffy, and C. Meade, *Phys. Rev. B* **50**, 13105 (1994).
- ²¹F. Birch, *J. Geophys. Res.* **83**, 1257 (1978).
- ²²K. Suito, M. Miyoshi, T. Sasakura, and H. Fujisawa, in *High-Pressure Research: Application to Earth and Planetary Sciences*, edited by Y. Syono and M. Manghnani (Terra Scientific, Tokyo, 1992), p. 219.
- ²³K. H. Smith, E. Shero, A. Chizmeshya, and G. H. Wolf, *J. Chem. Phys.* **102**, 6851 (1995).
- ²⁴O. B. Tsiok, V. V. Brazhkin, A. G. Lyapin, and L. G. Khvostantsev, *Phys. Rev. Lett.* **80**, 999 (1998).
- ²⁵J. P. Itie, A. Polian, G. Calas, J. Petiau, A. Fontaine, and H. Tolentino, *Phys. Rev. Lett.* **63**, 398LP (1989).
- ²⁶D. J. Durben and G. H. Wolf, *Phys. Rev. B* **43**, 2355LP (1991).
- ²⁷M. Grimsditch, R. Bhadra, and Y. Meng, *Phys. Rev. B* **38**, 7836 (1988).
- ²⁸G. H. Wolf, S. Wang, C. A. Herbst, D. J. Durben, W. F. Oliver, Z. C. Kang, and K. Halvorson, *High-Pressure Research: Application to Earth and Planetary Sciences* (American Geophysical Union, Washington, D.C., 1992), pp. 503–517.